Fibers and Polymers 2003, Vol.4, No.4, 188-194

Spinodal Phase Separation and Isothermal Crystallization Behavior in Blends of VDF/TrFE(75/25) Copolymer and Poly(1,4-butylene adipate) (I) -Spinodal Phase Separation Behavior-

Kap Jin Kim* and Thein Kyu[1]

Department of Polymer and Fiber Materials Engineering, College of Environment and Applied Chemistry, Kyung Hee University, Gyeonggi-do 449-701, Korea

[1]*Institute of Polymer Engineering, The University of Akron, Akron, OH44325-0301, USA*

(Received Novemver 11, 2003; Revised December 12, 2003; Accepted December 19, 2003)

Abstract: Phase behavior and spinodal phase separation kinetics in binary blends of a random copolymer of vinylidene fluoride and trifluoroethylene (75/25) [P(VDF/TrFE)] and poly(1,4-butylene adipate) (PBA) have been investigated by means of optical microscopic observation and time-resolved light scattering. The blends exhibited a typical lower critical solution temperature (LCST) ~34 °C above the melting temperature of the P(VDF/TrFE) crystals over the entire blend composition range. P(VDF/TrFE) and PBA were totally miscible in the temperature gap between the melting point of P(VDF/TrFE) and the LCST. Temperature jump experiments of the 3/7 P(VDF/TrFE)/PBA blend were carried out on a light-scattering apparatus from a single-phase melt state (180 °C) to a two-phase region (205~215 °C). Since the late stage of spinodal decomposition (SD) is prevalent in the 3/7 blend, SD was analyzed using a power law scheme. Self-similarity was preserved well in the late stage of SD in the 3/7 blend.

Keywords: P(VDF/TrFE), Poly(1,4-butylene adipate), Miscible blend, Spinodal phase separation

Introduction

Poly(vinylidene fluoride) [PVDF] with a strong C-F dipole moment is known to exhibit very good miscibility with poly (vinyl ester)s having pendant carbonyl groups due to dipole-dipole interaction or hydrogen bonding [1-3]. For instance, PVDF/poly(methyl methacrylate) [PMMA] and PVDF/poly (vinyl acetate) [PVAc] blends, which are miscible in the amorphous state over the entire blend compositions, exhibit a typical lower critical solution temperature (LCST) above the melting temperature of PVDF [1,2]. However, since LCST is higher than the thermal degradation temperature, no reports on the liquid-liquid phase separation kinetics of the blends have been found.

PVDF is also known to be miscible in the amorphous state with some semicrystalline polymers containing ester groups in their backbone chains such as poly(ε-caprolactone) [PCL] [4] and poly(pivalolactone) [PPVL] [5] due to specific interaction between fluorocarbon and ester groups. However, this kind of specific interaction weakens at elevated temperatures above the melting temperature of PVDF, resulting in liquid-liquid phase separation. In the PVDF/PCL blend, the LCST coexistence curve overlaps with the melting and/or crystallization curves over a wide composition range, thus phase separation and crystallization interfere with each other [4]. In the case of PVDF/PPVL blends [5], the LCST curve is located at extremely high temperatures, therefore thermal degradation may have occurred during the liquid-liquid phase separation.

Manley and co-workers [6-9] published a series of papers on miscibility, phase diagram, and crystallization behavior of a PVDF/poly(1,4-butylene adipate) (PBA) blend. The choice of their blend system has several advantages over other PVDF/semicrystalline polymer blends. First, the melting points of the constituents are about 100 °C apart, hence the melting and crystallization behavior occurring in both PVDF and PBA could be studied separately. Second, the observed LCST is located at ~60 °C above the melting temperature of the PVDF crystals, therefore the liquid-liquid phase separation behavior could also be studied without any interference from the melting transitions. However, since the spinodal phase separation temperature range of the PVDF/PBA blend is still high considering the thermal stability of PBA, one cannot exclude thermal degradation totally during the spinodal phase separation experiments.

Recently, in the PVDF/PBA blend system we replaced PVDF with a random copolymer of vinylidene fluoride and trifluoroethylene (75/25) [P(VDF/TrFE)], whose dipole moment is somewhat smaller than PVDF, thereby reducing the LCST to 185 °C (cf. the LCST of PVDF/PBA is 235 °C) [10]. Thermal degradation during the spinodal phase separation kinetics experiments will occur much less at these relatively moderate temperatures and the liquid-liquid spinodal phase separation kinetics of the P(VDF/TrFE)/PBA blend system can now be studied without degradation being a significant factor. Thus, we focused our attention on the spinodal phase separation kinetics of the 3/7 blend through T-jump from a single phase region to a two-phase region.

Experimental

The P(VDF/TrFE) copolymer of a molar ratio of 75/25 in

*Corresponding author: kjkim@khu.ac.kr

chip form, kindly supplied by Atochem Co., was used as-received. The PBA sample with a weight-average molecular weight (M_w) of 12 000 was purchased from Scientific Polymer Products, Inc. and used without further purification. P(VDF/TrFE) and PBA were dissolved separately in acetone. The 4 % acetone stock solutions were subsequently mixed in desired proportions. Film samples were cast on glass slide for light scattering and microscopic observation. The solvent was allowed to evaporate on a hot plate maintained at 50 °C for 30 min and the resulting films were further dried in vacuum at 80 °C for 3 days. In this way, blend samples were prepared in various compositions ranging from 90/10 to 10/90 by weight with 10 % increments; the first numeral refers to P(VDF/TrFE) composition.

All the thermal data on the melting transition, Curie transition, and glass transition were obtained with a Perkin-Elmer DSC-7 and a Du Pont DSC-9000. Details are described in a previous paper [10]. Cloud point of the P(VDF/TrFE)/PBA blends in the melt state was determined by measuring the scattering intensity at $\theta = 10°$ while heating at a rate of 0.5 °C/min. The temperature at which an abrupt increase in the scattered light intensity occurred in the course of heating due to binodal phase separation was regarded as the cloud point.

A time-resolved light scattering apparatus used in this study consists of a 5 mW He-Ne laser light source (05 LHR 151, Melles-Griot, the Netherlands) with a wavelength of 632.8 nm, a customer-made hot stage controlled by a programmable temperature controller (CN2001, Omega Technologies Co, U.S.A.), a screen made of white tracing paper, and a 2-D CCD camera(Orbis16, pixels 1280 × 1024, 16 bit resolution, SpetraSource Instruments, U.S.A.). The scattered light intensity data in one dimension along the scattering angle measured by the CCD camera as a function of time were automatically sent to a PC and saved for further analysis. For temperature (T) jump experiments, an additional hot stage was used for preheating a specimen at a single-phase temperature of 180 °C. The specimen was rapidly transferred from the preheating hot stage to the hot stage on the light scattering apparatus with a second then kept at the desired spinodal phase separation temperature. The temperature equilibrates within about 2-3 s, after it drops initially by 1-2 degrees.

Results and Discussion

Phase Behavior

Figure 1 shows the overall phase diagram of the P(VDF/TrFE)/PBA blend system. Pure PBA exhibits only two phase transitions, i.e. glass transition (T_g) and melting (T_m), whereas the neat VDF/TrFE copolymer shows three phase transitions, i.e. glass transition, melting, and Curie transition. With a large hysteresis, the Curie transition from paraelectric-to-ferroelectric ($T_{P \Rightarrow F} = 60$ °C) and vice versa ferroelectric-to-paraelectric transition ($T_{F \Rightarrow P} = 112$ °C) occur reversibly

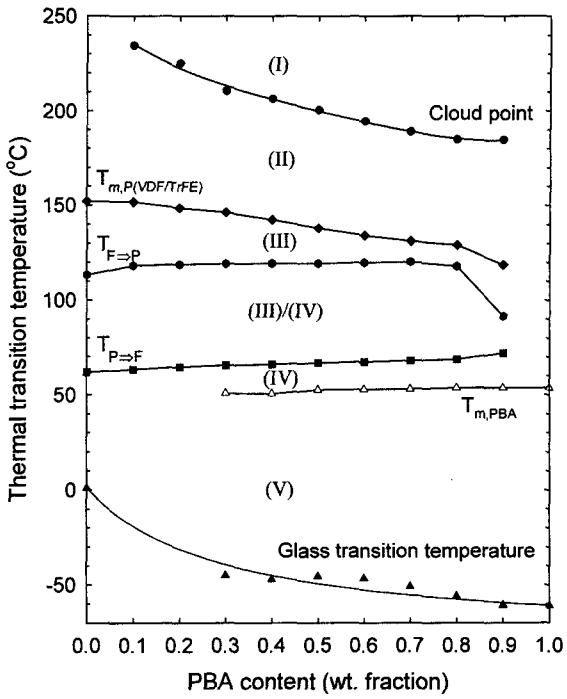

Figure 1. Phase diagram of P(VDF/TrFE)/PBA blends.

during cooling and heating. The intermediate blends undergo more complex phase transitions, showing a single glass transition, two melting transitions, Curie transition, and liquid-liquid phase separation above the lower critical solution temperature (LCST). P(VDF/TrFE) and PBA are miscible in the temperature gap between the melting point of P(VDF/TrFE) and the LCST. Raising the temperature of the blend from a single phase region (region II) to an immiscible gap (region I) eventually leads to liquid-liquid phase separation associated with the reduction in the contribution of the specific interaction between the polar groups of the constituents. The observation of two distinct melting points, i.e., at ~54 °C for PBA and at ~151 °C for P(VDF/TrFE), indicates that the two polymers crystallize separately. In a previous paper, a value for the Flory-Huggins interaction parameter of $\chi_{12} = -0.592$ (at 160 °C), which suggests that the two polymers are thermodynamically miscible in the melt, was calculated from the melting point depression of P(VDF/TrFE) in the P(VDF/TrFE)/PBA blend system [10].

Figure 2 shows the LCST cloud point phase diagram with a minimum around 80 wt% PBA ($\phi_2 = 0.84$). The fact that the LCST minimum is located at an extremely high PBA composition implies that the molecular weight of the P(VDF/TrFE) must be significantly higher than that of PBA. Under the assumption that the measured cloud points are very near binodal decomposition temperatures, the cloud points were fitted with the binodal points calculated on the basis of the Flory-Huggins equation [11],

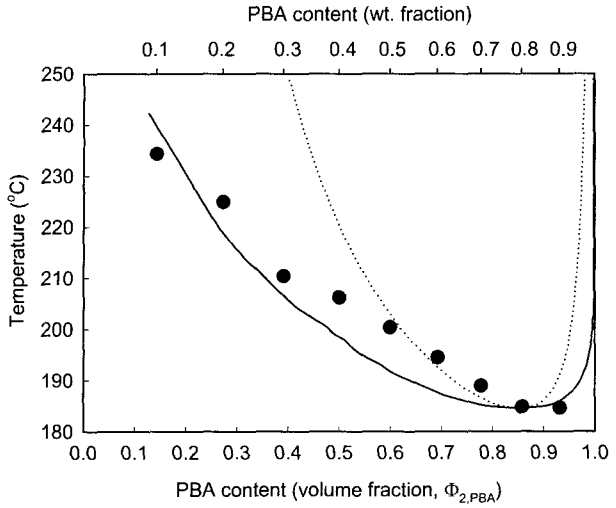

Figure 2. The fitted binodal and spinodal decomposition lines of P(VDF/TrFE)/PBA blends calculated based on Flory-Huggins theory in comparison with the experimental cloud point phase diagram.

$$(\Delta G_m)/V = RT\left(\frac{\phi_1}{V_1}\ln\phi_1 + \frac{\phi_2}{V_2}\ln\phi_2 + \chi\phi_1\phi_2\right) \quad (1)$$

where $\Delta G_m/V$ is the free energy of mixing per unit volume of the mixture, ϕ_i is the volume fraction of the i^{th} polymer, V_i is the molar volume of the i^{th} polymer, subscripts 1 and 2 represent P(VDF/TrFE) and PBA, respectively. V_i is obtained from the following relation;

$$V_i = MW_i \times V_{i,sp} \quad (2)$$

where MW_i and $V_{i,sp}$ are the molecular weight and specific volume of the i^{th} polymer, respectively. $V_{1,sp} = 0.5419$ cm^3/g and $V_{2,sp} = 0.9813$ cm^3/g. The interaction parameter χ is now assumed to be dependent on temperature and composition as follows;

$$\chi = a + b/T + c\phi_2/T \quad (3)$$

Since c is generally negligibly small compared with parameters a and b, c was assumed to be zero in this study. The best-fitted binodal line could be obtained as seen in Figure 2 with $a = 0.00055$, $b = -0.21935$, and $MW_1 = 600\,000$. In this non-linear least-squares curve-fit, we did not consider the effect of temperature on the volume fraction to simplify calculation. The calculated binodal line is seen to agree well with the experimental cloud points, showing that it can be used to obtain a rough prediction of the spinodal line, which can then be utilized as a reference in the phase separation kinetic experiments of the P(VDF/TrFE)/PBA blends. Thus the minimum jumping temperature adopted for spinodal phase separation of 3/7 blend were chosen as 205 °C. This temperature is located 15 °C above the spinodal point.

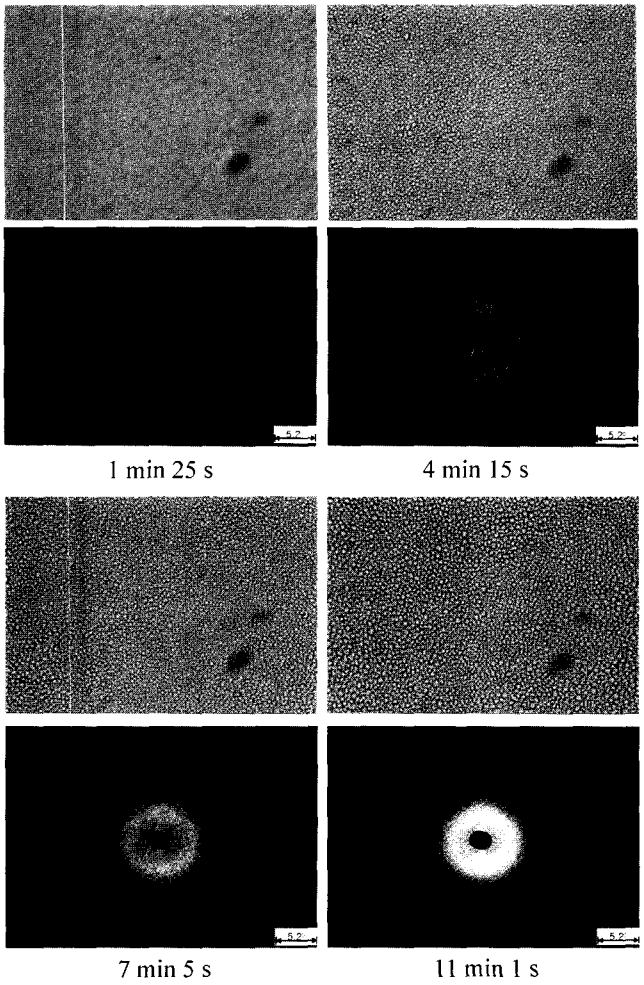

Figure 3. Optical micrographs of the 3/7 blend revealing interconnected domains and the corresponding scattering halo during spinodal decomposition following a T jump from 180 °C to 205 °C.

When the 3/7 blend in a single phase at 180 °C is suddenly heated to an unstable two-phase region at 205 °C, a highly interconnected structure can be observed under an optical microscope. The size of phase-separated domain gets larger with time. In laser light scattering measurements, a scattering halo corresponding to the average periodic distance of the phase-separated domains develops and then collapses to a smaller diameter with demixing time. Figure 3 shows optical micrographs and light scattering halos of the 3/7 blend with phase-separation time. Figure 4 shows the rapid decay of the scattering intensity with time following T quench from 225 °C to 150 °C, which is above the melting temperature of P(VDF /TrFE) in the 5/5 blend, indicating that phase dissolution is nearly completed within 180 s. This result confirms that the observed LCST is thermally reversible, which is the prerequisite for a true LCST.

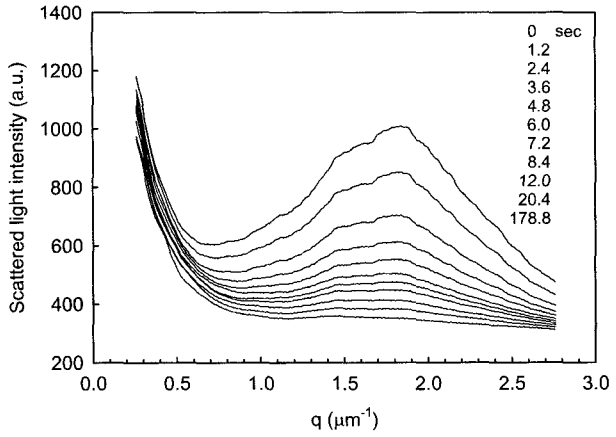

Figure 4. Time decay of scattering curves of the 5/5 blend following a reverse T quench from a two-phase (225 °C) to a single-phase melt state (150 °C) exhibiting phase dissolution.

Kinetics of Spinodal Phase Separation

Figure 5 shows the time evolution of scattering profiles from a single-phase (180 °C) to a two-phase region (205~215 °C) for the 3/7 blend. Here, the scattered light intensity I is shown as a function of the scattering vector q [= $(4\pi/\lambda)\sin(\theta/2)$ where λ is the wavelength of light in the specimen and θ is the scattering angle]. In all the temperature jump experiments, there is no discernible period that can be characterized as the early stage of spinodal decomposition (SD) where the scattered light intensity increases gradually without a shift in the peak maximum q_m, whereas the phase separation shows a typical intermediate or late stage of SD, i.e., the peak maximum is shifted to a lower wavenumber as the scattered intensity increases gradually with elapsed time. The increasing rate of spinodal phase separation with increasing annealing temperature is attributed to the reduction in viscosity as well as an increase in thermodynamic instability.

In the late stage of SD, a scaling law suggesting the similarity of a structure factor $S(q, t)$ at later times to that of earlier times governs a nonequilibrium dynamical evolution toward thermodynamic equilibrium [12]. Binder and Stauffer assumed that clusters aggregate by a diffusion process and coalesce into larger clusters and described the self-similar growth of the structure by the power law scheme;

$$q_m(t) = 2\pi/\Lambda(t) \propto t^{-\alpha} \tag{4}$$

and

$$I_m(t) \propto \langle \eta(t)^2 \rangle \Lambda(t)^3 \propto t^{\beta} \tag{5}$$

where I_m is the scattered light intensity at q_m. $\langle \eta(t)^2 \rangle$ and $\Lambda(t)$ represent the mean-squared fluctuation of refractive indices and the length scale of the separated domains, respectively. The exponents, α and β, have been predicted by various theories. Langer, Baron, and Miller (LBM) calculated $\alpha = 0$ for the early regime and $\alpha = 0.21$ for the later coarsening based on the nonlinear scheme [13]. Binder and Stauffer predicted $\alpha = 1/(3 + d)$ for the low-temperature regime, with d being the dimensionality of growth based on the cluster reaction [12]. Later, Binder obtained $\alpha = 1/(2 + d)$ for an intermediate regime after a complicated initial stage and $\beta = 3\alpha$ at late stages with $\alpha = 1/3$ and $\beta = 1$ for fluid mixture [14]. The notable values $\alpha = 1/3$ and $\beta = 1$ for the late stages of SD for solid mixtures were also predicted by the classical evaporation-condensation mechanism (or Ostwald ripening mechanism) proposed by Lifshitz and Slyozov [15]. On the other hand, Siggia obtained a similar relationship, but with $\alpha = 1/3$ for the intermediate state and $\alpha = 1$ for the late stage of SD of a critical mixture where the motion of the interface driven by the interfacial tension must be taken into account [16].

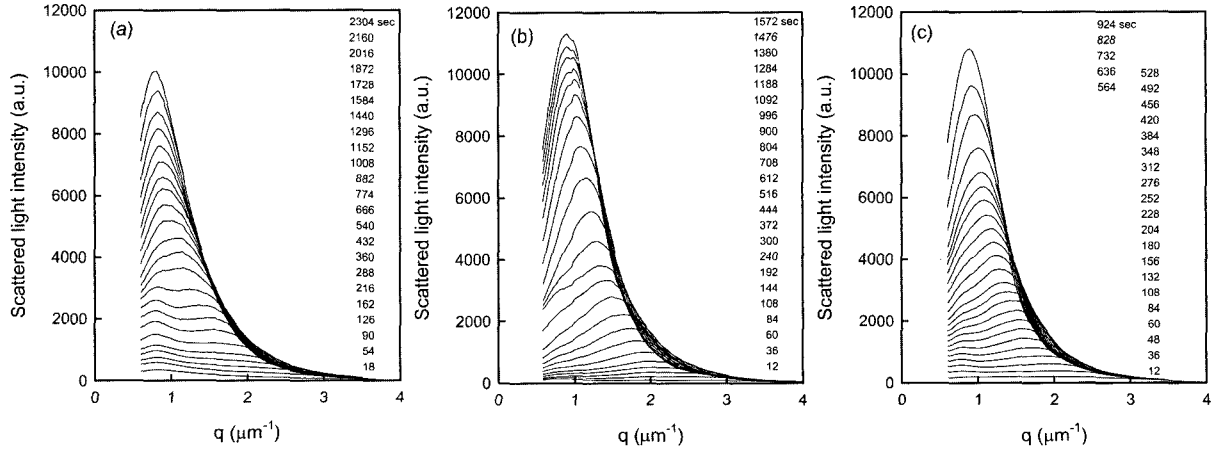

Figure 5. Time evolution of scattering profiles of the 3/7 blend after temperature jumps from a single-phase in the melt (180 °C) to two-phase temperatures (a) 205, (b) 210, and (c) 215 °C.

Figure 6(a) and (b) show the log-log plots of the maximum wavenumber q_m and the corresponding scattered light intensity maximum I_m versus phase separation time for the 3/7 blend, respectively. In the case of the spinodal phase separation of the 3/7 blend, the exponent values ($\alpha = 1/3$, $\beta = 1$, and $\beta = 3\alpha$) agree very well with the dynamics of cluster coalescence for fluid mixtures suggested by Binder and Stauffer [12,14] and with the evaporation-condensation mechanism for solid mixtures proposed by Lifshitz and Slyozov [15] for the late stage of SD. The equality of $\beta = 3\alpha$ in the late stage is a consequence of the coarsening process and dynamics being scaled with a single length parameter $\Lambda(t)$; the amplitude of the fluctuation reaching at the thermodynamic equilibrium value and only the wavelength of the fluctuations increases according to equation (4). Although the phase separation time is sufficiently long for the 3/7 blend, the percolation regime ($\alpha = 1$), where flow takes place through interconnected channels between domains due to the coarsening process driven by the interfacial tension as suggested by Siggia [16], is never reached.

Scaling Tests of Spinodal Phase Separation

The growth of phase-separated domains involves a change in length scale (size) as well as in structure (shape). The scattered light intensity $I(q, t)$ for the three-dimensional growth of phase-separated domains can be expressed as

$$I(q, t) \sim V\langle \eta(t)^2 \rangle \xi(t)^3 S[q\xi(t)] \tag{6}$$

where V is the scattering volume, $\langle \eta(t)^2 \rangle$ is the mean-square fluctuation of refractive indices, $\xi(t)$ is the correlation length, which relates to the wavelength of periodic structure $\Lambda(t)$, i.e., $\xi(t) = \Lambda(t)/2\pi = 1/q_m(t)$, $q\xi(t)$ is the reduced scattering vector, equaling $q/q_m(t)$, and $S[q\xi(t)]$ is the scaled structure factor.

In the late stage of spinodal phase separation where $\langle \eta(t)^2 \rangle$ reaches a constant equilibrium value, $I(q, t)$ can be scaled with a single time-dependent length parameter $\xi(t)$. Therefore,

$$S[q\xi(t)] = S(x) \sim I(q,t)q_m(t)^3 \equiv F(x) \tag{7}$$

can be obtained with $x = q\xi(t) = q/q_m(t)$, i.e., self-similarity can be preserved. However, since in the early to intermediate stage both $\langle \eta(t)^2 \rangle$ and $\xi(t)$ change with time t, $I(q, t)$ cannot be scaled with a single length parameter and $F(x)$ cannot be obtained from $I(q, t)$, i.e., self-similarity cannot be preserved.

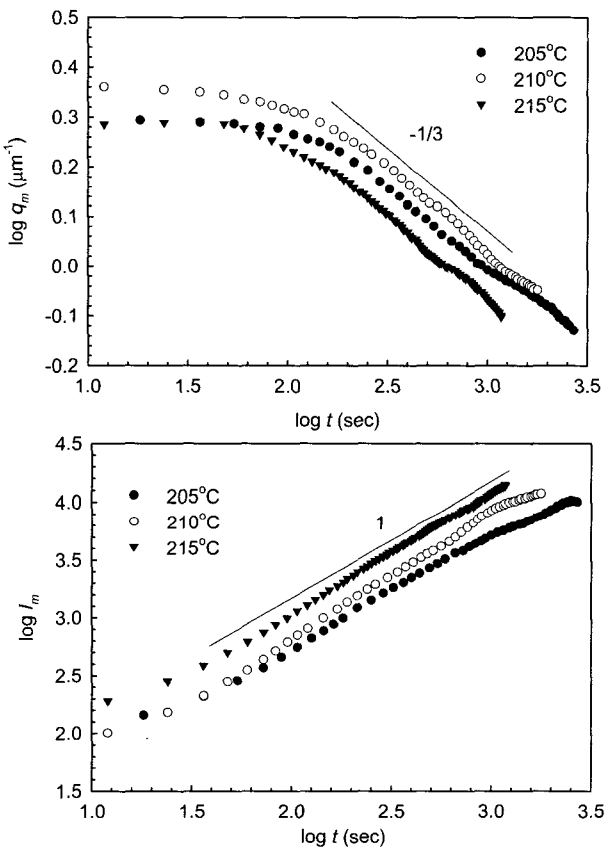

Figure 6. log-log plots of (a) $q_m \sim t^{-\alpha}$ and (b) $I_m \sim t^{\beta}$ following a T jump from 180 to 205, 210, and 215 °C for the 3/7 blend.

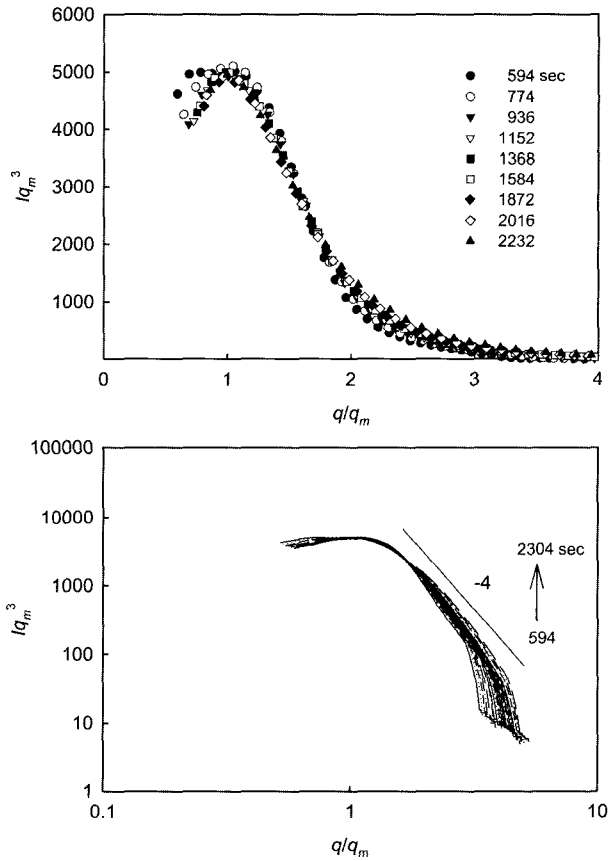

Figure 7(a). Self-similarity test for the 3/7 blend following a T jump from 180 °C to 205 °C.

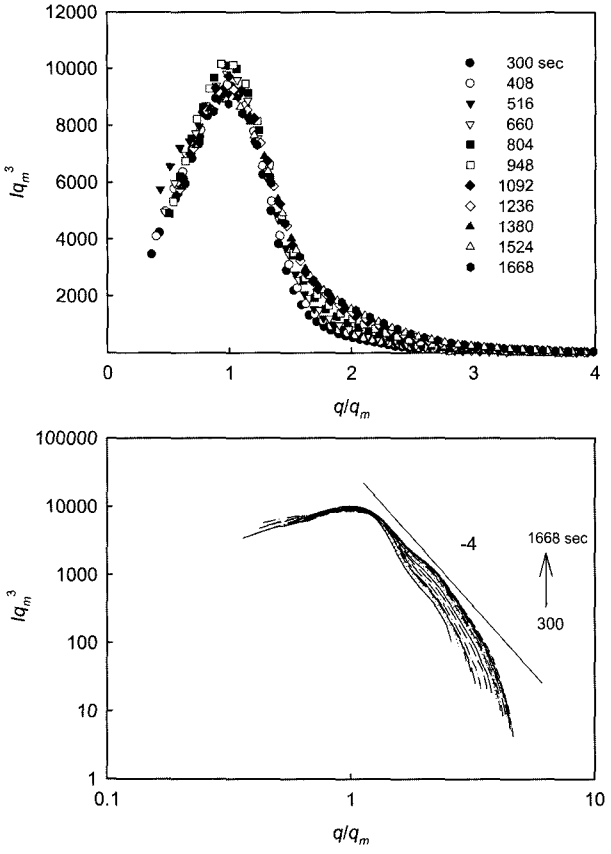

Figure 7(b). Self-similarity test for the 3/7 blend following a T jump from 180 °C to 210 °C.

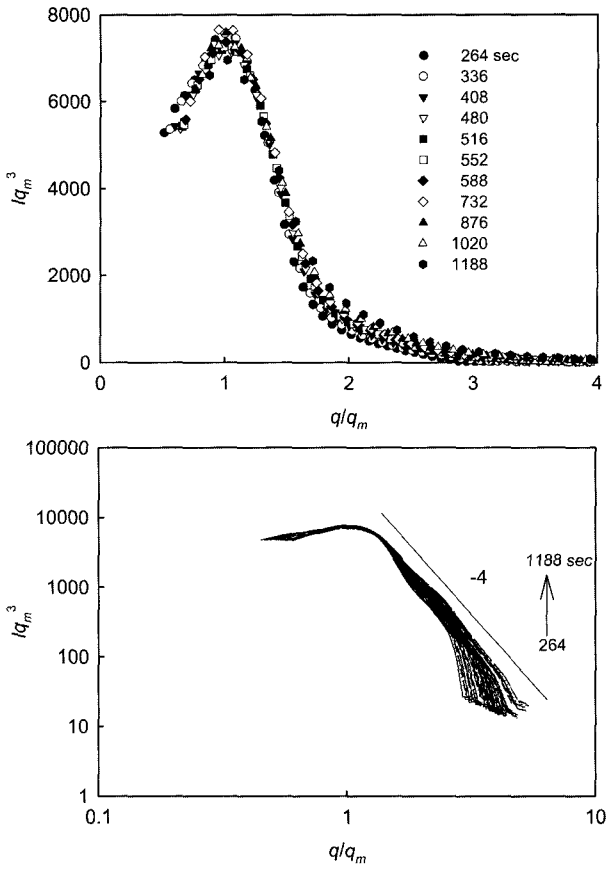

Figure 7(c). Self-similarity test for the 3/7 blend following a T jump from 180 °C to 215 °C.

Therefore, we employed the data of SD of the 3/7 blend, where the late stage is dominant during spinodal phase separation, for this scaling test.

As shown in the upper part of Figure 7, the $F(x)$ vs x plot (i.e., Iq_m^3 vs q/q_m plot) shows a good superposition for different phase separation times, suggesting that self-similarity can be attained as the structure function exhibits temporal universality. There is no difference in the behavior of scaled structure functions for different T jumps, as long as the time scale is in the universal region.

To get additional information on the intricate local structure such as interface sharpness, it is necessary to investigate in detail the $F(x)$ at larger x regions. The shape of the structure factor $F(x)$, which may be scaled by a single length parameter in the late stage of SD, was analyzed by Furukawa [17] as follows:

$$F(x) = (1 + \gamma/2)x^2/(\gamma/2 + x^{2+\gamma}) \quad (8)$$

where $\gamma = 1 + d$ for an off-critical mixture and $\gamma = 2d$ for a critical mixture; d is the dimensionality of growth. For three-dimensional growth, $F(x) \sim x^2$ for $x < 1$, and for $x > 1$, $F(x) \sim x^{-6}$ (for a critical mixture) and $F(x) \sim x^{-4}$ (for an off-critical mixture). The bottoms of Figure 7(a)~(c) show the log-log plots of Iq_m^3 vs q/q_m. The value of slope for $x > 1$ is approximately -4, suggesting that the SD process of the 3/7 blend is reminiscent of the behavior of off-critical mixtures as shown in Figure 2 representing the fitted binodal and spinodal lines.

Conclusions

The blends of P(VDF/TrFE)/PBA showed a typical LCST ~34 °C above the melting temperature of the P(VDF/TrFE) crystals, and were miscible in a temperature gap between the melting point of P(VDF/TrFE) and the LCST over the entire blend composition range. Time-resolved light scattering experiments following a T jump from a melt single phase to a two-phase region showed that the late stage of SD is prevalent in the 3/7 blend. The intermediate and late stages of SD could be analyzed with a power law scheme ($q_m(t) \propto t^{-\alpha}$ and $I_m(t) \propto t^{\beta}$). Since, in the late stage of SD where $\langle \eta(t)^2 \rangle$ reaches a constant equilibrium value, $I(q, t)$ can be scaled with a single time-dependent length parameter $\xi(t)$. Thus self-similarity was preserved well in the late stage of SD in the 3/7 blend.

Acknowledgements

One of the authors (KJK) greatly appreciates financial support from Korea Research Foundation (KRF-99-041-E00406).

References

1. D. R. Paul, J. W. Barlow, R. E. Bernstein, and D. C.Wahrmund, *Polym. Eng. Sci.*, **18**, 1225 (1978).
2. H. Tomura, H. Saito, and T. Inoue, *Macromolecules*, **25**, 1661 (1992).
3. K. J. Kim, Y. S. Rho, and D. H. Choi, *J. Korean Fiber Soc.*, **34**, 304 (1997).
4. W. H. Jo, S. J. Park, and I. H. Kwon, *Polym. International*, **29**, 173 (1992).
5. J. Huang, A. Prasad, and H. Marand, *Polymer*, **35**, 1896 (1994).
6. J. P. Penning and R. St. J. Manley, *Macromolecules*, **29**, 77 (1996).
7. J. P. Penning and R. St. J. Manley, *Macromolecules*, **29**, 84 (1996).
8. K. Fujita, T. Kyu, and R. St. J. Manley, *Macromolecules*, **29**, 91 (1996).
9. L.-Z. Liu, B. Chu, J. P. Penning, and R. St. J. Manley, *Macromolecules*, **30**, 4398 (1997).
10. K. J. Kim and T. Kyu, *Polymer*, **40**, 6125 (1999).
11. O. Olabisi, L. M. Robeson, and M. T. Shaw, "Polymer-Polymer Miscibility", Chap. 2, Academic Press, New York, 1979.
12. K. Binder and D. Stauffer, *Phys. Rev. Lett.*, **33**, 1006 (1973).
13. J. S. Langer, M. Baron, and H. S. Miller, *Phys. Rev. A*, **11**, 1417 (1975).
14. K. Binder, *Phys. Rev. B*, **15**, 4425 (1977).
15. I. M. Lifshitz and V. V. Slyozov, *J. Phys. Chem. Solids*, **19**, 35 (1961).
16. E. D. Siggia, *Phys. Rev. A*, **20**, 595 (1979).
17. H. Furukawa, *Physica A*, **123**, 497 (1984).